FACULTY OF INFORMATION TECHNOLOGY AND ELECTRICAL ENGINEERING

DEGREE PROGRAMME IN WIRELESS COMMUNICATIONS ENGINEERING

MASTER'S THESIS

Impact of Mechanical Vibration on Over-the-Air Link at Upper mmW Frequencies

Author	Mohammad Faijus Salehin
Supervisor	Dr. Marko E. Leinonen
Second Examiner	Prof. Dr. Aarno Pärssinen
Technical Advisor	Dr. Marko E. Leinonen

August 2022

Mohammad Faijus Salehin (2022) Impact of Mechanical Vibration on Over-the-Air Link at Upper mmW Frequencies. The University of Oulu, Faculty of Information Technology and Electrical Engineering, Degree Program in Wireless Communications Engineering. Master's Thesis, 39 p.

ABSTRACT

Mechanical vibrations will affect the performance of the wireless link especially with coming 6G systems, which will operate at significantly higher frequencies than current 5G networks. The mechanical vibrations affect the frequency generation circuitries of the radio equipment and thus the performance of the radio link. The amount of mechanical vibration to the radio or any equipment has been standardized and a short summary of related standards has been given in the thesis.

Some practical measurements have been performed to verify the effects of mechanical vibration on wireless link performance. The measurement has been done with a vector signal analyzer that measures the S-parameters of the wireless link. The phase response of the measured S-parameters has been studied to illustrate the phenomena.

The mechanical vibration has been measured with a mobile phone application which detects the changes, vibrations, and location changes of the mobile phone when it was placed over the frequency extender. As a result of the selection of frequency extenders, the RF measurement equipment has been able to perform over a greater frequency range than was originally intended. The used mobile phone application was the G-force meter, which is freely available from application stores.

The measured S-parameters S11 and S21 were analyzed with Matlab software which was provided for the purpose. The measured S-parameters and vibration results have been time synchronized in the Matlab result post-processing. The measurement results show clearly that mechanical vibrations influence the radio signal phase and thus it needs to be considered in the future development of 6G.

Keywords: VNA, PNA, S-parameters, RF, THz radios, millimeter-wave(mmW).

TABLE OF CONTENTS

ABSTRACT
TABLE OF CONTENTS
FOREWORD
LIST OF ABBREVIATIONS AND SYMBOLS
1 INTRODUCTION 6
1.1 6G system 6
1.2 Vibration with mobile equipment 7
2 EFFECTS OF MECHANICAL VIBRATION TO ELECTRICAL PARAMETERS 9
2.1 Mechanical vibrations models and standards 9
2.2 Mechanical vibrations in the mobile terminal 9
2.3 Mechanical vibration effects on oscillators 10
3 VALIDATION MEASUREMENT SET-UP 13
3.1 Measurement setup with mechanical vibration 13
3.2 Network Analyzer for S-parameter measurement 15
3.3 Frequency extenders 16
3.3.1 Used Frequency Extender connections 17
3.4 Calibration 19
3.4.1 Calibration Kit 19
3.4.1 Calibration, Extenders back-to-back 20
3.4.1 Calibration with Quarter wave Offset shim 21
3.4.2 Enhanced Response Calibration 22
4 MEASUREMENT RESULTS OF VIBRATION TESTS WITH 140 GHZ SIGNAL 23
4.1 Vibration with back-to-back extenders 23
4.2 Vibration at receiver side with OTA link 25
4.3 Fast Vibration at transmitter side with OTA link 28
4.4 Higher OTA link level vibration at transmitter side with OTA link 31
5 DISCUSSION 36
6 SUMMARY 37
7 REFERENCES 38

FOREWORD

An old proverb states It is as important for a man to have an aim in life for purpose as it is for a ship without a radar. Hence, I had the aimed to be an M.Sc. (Tech.). At the University of Oulu, the work on the thesis was completed as part of the master's degree requirements in wireless communications engineering, which is part of the M.Sc. of Technology (Technology). In the field of wireless communications engineering, there are several requirements. Firstly, I would like to express my sincere gratitude to the Centre for Wireless Communications as well as the University of Oulu, which created an academic platform and learning environment that would allow me to think and grasp tangible things behind the scenes that are out of the box and enhance my skill set.

Throughout my master's thesis journey, I would like to take this opportunity to express my sincere gratitude to my technical advisor Dr. Marko E. Leinonen. He provided me with direct support throughout the entire duration of my journey. I want to thank you for your guidance at each stage of the process, as it enabled us to complete the work on time. Additionally, I would like to express my gratitude to my supervisors, Dr. Marko E. Leinonen and Prof. Dr. Aarno Pärssinen. These supervisors have provided wonderful ideas which led to the completion of this thesis. My thesis would not have been possible without the support, comments, and reviews that you both provided.

As a student, I am grateful for all the support and love that I have received from my family members during my university studies. I would especially like to thank my best friend, Humayun Rashid Chowdhury, and my another friend Tamzed Anwar. They always spent time with me and always made me feel at ease. Furthermore, I would like to extend my gratitude and regards from the bottom of my heart to my younger brother Ainus Salehin and my lovely wife, Farjana Salehin. It has been a pleasure to have her support over the years as we have pursued our passions through Skype, and she has always been by my side. Also, I would like to express my sincere appreciation to my daughter, Aleeza Salehin, for all that she has done for me. I am giving her endless pleasure and happiness by having her write my dissertation in Bangladesh. I dedicate my dedication to the unconditional love, encouragement, and support of my mother, Hosne Ara Begum, and my father, Mohammad Motaher Hossain. In addition, I would like to express my gratitude to the Finnish education authority for providing me with the opportunity to pursue my master's degree through their educational system. I was also inspired by Dr. Shahriar Shahabuddin when it came to realizing my dreams. In my case, I am a patient suffering from a Brain Hemorrhage, and I had the pleasure of being observed by three doctors during my treatment. Shahin Afroz Orin, Farah Tazkera Rahman, and Mirva Natyänki. Special thanks to them. To achieve this result, I have put a lot of effort, hard work, dedication, and effort that goes into my endeavors. All that things belong to my Almighty ALLAH. ALLHAMDULILAH for everything.

Oulu, Finland, August 2022
Mohammad Faijus Salehin

LIST OF ABBREVIATIONS AND SYMBOLS

3GPP	3rd generation partnership program
5G	5th generation mobile network
5GTN	5G test network
6G	6th generation mobile network
ETSI	European Telecommunications Standards Institute
F5G	fifth generation fixed network
FIR	finite impulse response
FDMA	frequency division multiple access
FR1	frequency range 1
FR2	frequency range 2
GHz	gigahertz
HF	high frequency
IP	internet protocol
ISO	International Standards Organization
Km	kilometre
LAN	local area network
LO	local oscillator
LOS	line of sight
MIMO	multiple input multiple output
mmW	millimeter-wave
MHz	megahertz
OTA	over-the-air
PFD	phase frequency detector
PLL	phase locked Loop
PON	passive optical network
PN	phase Noise
PNA	performance network analyzer
PM	phase modulation
QCS	quartz crystal oscillator
RF	radiofrequency
Rx	receiver
RX	reception
S-parameters	scattering parameters
THRU	through
TX	transmission
TRX	transceiver
TX	transmitter
THz	terahertz
VNA	vector network analyzer
VCXO	voltage-controlled crystal oscillator

1 INTRODUCTION

1.1 6G system

In 2019, the fifth generation(5G) technology standard for broadband cellular networks began to deploy worldwide. Both the uplink (UL) and the downlink (DL) of 5G systems are based on the OFDMA (Orthogonal Frequency Division Multiple Access) standards. Several frequencies have been used for 5G networks, such as the first frequency range (FR1), between 450 MHz and 6 GHz, and the second frequency range (FR2), between 24.25 GHz and 52.6 GHz. [1]

To make use of upcoming next-generation technologies such as Wi-Fi 7, 50G PON (passive optical network), and 800G, the fixed networks must be upgraded to support 6G. The intermediate step between 5G and 6G is the fifth-generation fixed network and F5.5G, which provides improved access to homes between 1 Gbps and 10 Gbps around the world. There is also a possibility that network capabilities will go beyond the level of telecommunications into the industrial sphere. Taking advantage of the F5.5G is that network latency will be reduced to microseconds, allowing industrial robots to be controlled instantly. As a result of the deployment of F5.5G, network reliability can be improved from 99.99% to 99.9999%, which enables high-frequency power grid dispatching to become more efficient. Lastly, F5.5G will take optical communication one step further by providing optical sensing systems that can detect vibration, stress, temperature, and others through fiber scattering. This will improve positioning accuracy to approximately one meter of the device's location. Due to the low energy consumption associated with optical technology, F5.5G is expected to boost network energy efficiency by 10-fold compared with current technologies. It is expected that the 6G network will have air latency of fewer than 100 microseconds and will operate at terahertz frequency bands, capable of transmitting data at a peak speed of 1,000 gigabits per second. [2]

Some differences need to be noted in the case of 5G and 6G networks. It is expected that the 6G networking data speed will be 100 times faster than the 5G networking data speed and offer greater reliability and a wider network coverage than the 5G networks. Due to the limited bandwidth available for 6G at currently used frequency bands, higher frequencies are required for operation. In the coming years, it is likely that the frequency band, overlapping upper millimeter wave (mmW) frequencies of 100 to 300 GHz, will be the most important band for researching new radio communications systems. In the coming years. The significantly greater region of spectrum available in this region than in the lower mmW region already used by 5G FR2 (24 - 48 GHz). A few techniques are being used to achieve a very high spectral efficiency at frequencies below 5G FR1 frequencies such as 5G, including Orthogonal Frequency Division Multiplexing (OFDM) and sophisticated communications schemes, e.g., high order Multiple Input Multiple Output (MIMO). High-efficiency modulation schemes and high-order MIMO used for high data rates are impossible to implement at FR1 for 6G because of the scarcity of available bandwidth.[3]

1.2 Vibration with mobile equipment

When a user is walking, we are having problems with the mobile vibrating when the body of the user is vibrating, so the mobile is shaking. As shown in Figure 1, the user experiences up-and-down movements during their walking, and the same is true for the radio equipment as well, which can be seen in Figure 1. Similarly, when driving on the road with small bumps, in-vehicle communication starts to malfunction when there are small bumps in the road. The problems are caused by the mobile vibrating, which in turn causes the body to vibrate. These effects lead to the Doppler shift and fluctuations in the signal level. As a result, when it comes to different speeds, several factors must be considered, most importantly the deployment and operation scenarios. A test vehicle for 6G drive testing is shown in Figure 2.

As part of our 5G solutions, we should be able to support mobility on demand, ranging from very high mobility, such as high-speed trains and airplanes, to very low mobility, such as smart meters. Although there is a requirement to have different speeds depending on the deployment and operation scenarios, the main requirement is different speeds. The main challenge of a seamless wide-area cover scenario is to provide users with a user-experienced data rate of around 100 Mbps at any time and place, even if they are traveling at high speeds (500 km/h). The most important performance indicators assessed under the highway deployment scenario would be the reliability, the design, the analysis, and the evaluation of the 5G network. It is, therefore, necessary to have automatic gain control at both the transmitter and receiver ends. It offers accurate channel estimation, advanced signal processing, optimal network deployment, and effective channel deployment. The small mobility observed in 6G systems at high frequencies corresponds to the high mobility observed at lower frequencies in 6G systems.[4]

Figure 1. While walking, In this Figure 1, we can see an example of what I mean. The mobile phone vibrates due to up and down movements and down movement of the mobile phone.

Figure 2. Car can experience to up and down movement while driving at road.

2 EFFECTS OF MECHANICAL VIBRATION TO ELECTRICAL PARAMETERS

Since vibration affects electrical components, vibration tolerance is specified in multiple standards for electrical components and mechanical sub-assemblies. The following sub-chapters provide some examples of how this can be achieved.

2.1 Mechanical vibrations models and standards

It is important to note that several standards are specified for mechanical vibrations. For example, the operation of any telecommunication base station in a building is limited by a long-term structural monitoring system concerning the vibrations induced by the base station itself. There is a possibility that construction sites can generate a high level of vibration due to the construction process and the use of heavy equipment during the construction process. This can cause a disturbance, limit certain activities, and damage buildings, especially if the area is densely populated. An example of a monitoring campaign started in 2014 to verify whether vibration was generated during the construction of a 19-floor 50,000 square meter building located adjacent to the monitored building, fixing telecommunication equipment was divided into two phases. As part of the project, standards for vibration were specified. The first standard is for velocity tests conducted according to DIN-4150-3, and the double standard is ETSI EN 300019-1-3, which includes the maximum acceleration of telecommunications equipment.[5]

To minimize the effects vibrations could have on a building's structural integrity, the DIN-4150-3 standard compares the vibration velocity and frequency measured on the building's structure with recommended limit values.

Following ETSI EN 300019-1-3, vibration monitoring for telecommunications equipment specifies the environmental conditions that the equipment must be in. It defines the environmental conditions that telecommunications equipment may be exposed to, as well as the severity of these conditions. [5]

2.2 Mechanical vibrations in the mobile terminal

Mechanical vibration can be used to improve the limited user interface of a mobile device when those are generated inside the mobile. A vibration rendering can enhance the identification of mobile device vibrations produced by a vibration motor. Transparent rendering can contribute to increasing the number of discrete vibrations used for information delivery via a mobile device. [6]

It is imperative to realize that mechanical vibrations can positively affect the limited user interface of a mobile device when generated within the device. It can be beneficial to use vibration rendering to enhance the ability to identify vibrations produced by motion motors in

mobile devices. There is a possibility that transparent rendering can contribute to an increase in the number of discrete vibrations that can be used to convey information through mobile devices. This is because transparent rendering uses transparent rendering.[7]

There is also an alternative sensor module that is battery-less and uses piezoelectric energy converters for converting mechanical vibrations into electricity that is used to supply energy for RF transmission through a wireless system.[8]

2.3 Mechanical vibration effects on oscillators

In telecommunications, industry professionals agree that the local oscillator plays a major role in determining the overall phase noise of the system. Crystals, which generate a base clock, are vibrated by mechanical vibrations. When the mechanical vibrations are added to the oscillator's phase noise, the noise gets amplified at the output of the transmitter or receiver. Vibrations produce physical phase modulation because of kinetic motion. There is an increase in the noise of oscillators because of mechanical vibration-induced phase modulation (PM).[10]

In recent years, the crystal oscillator has been the system's most widely used frequency base in radio communications. With varying forces and frequencies of vibration, the crystal oscillator is vibrated at a constant frequency as it vibrates, affecting the signal's phase noise. It should be noted that as phase noise also decreases, the signal-to-noise ratio also increases. It is likely that the probability of receiving or transmitting an incorrect signal increase as the quality of power of the transmission decreases. Therefore, it is very important to limit the phase noise increase that occurs as the operating frequency of the equipment or instrument is being used in the system. The electronic oscillators must provide a sufficiently low level of phase modulation (PM) noise to satisfy the system requirements, regardless of the environment in which it is installed. On the other hand, mechanical vibrations and accelerations can introduce mechanical deformations into oscillators, which lead to an increase in the oscillator's otherwise low PM noise. There is a relationship between the phase noise stability of an oscillator and the degradation of the performance of an electronic system. There is no doubt that vibrations are undesirable for oscillators with low noise levels. A high-precision oscillator is a vital component of modern communication and navigation systems, radars, and sensors mounted on uncrewed aerial vehicles, helicopters, missiles, and other dynamic platforms that rely on communications. [11]

The frequency change of an oscillator can be reduced by applying compensation that reduces the frequency change caused by vibrations on an oscillator. An oscillator with and without compensation must be studied in terms of phase noise to be able to compare its performance with that of an oscillator without compensation to evaluate the performance of the oscillator. As a result of using this compensation system, any communication system currently being used that utilizes crystal oscillators will have less phase noise overall compared to systems that do not use it. If the PM noise in the operating system is kept as low as possible, then oscillators can often satisfy the system requirements in static conditions. Phase fluctuations within its cause an oscillator's sensitivity to vibration. positive feedback

Loop, which contributes to the time-frequency oscillator's sensitivity to vibration. The industry has implemented mechanical isolation systems to limit the propagation of mechanical vibrations to the frequency standard. This prevents the system from deviating significantly from its frequency standard. As a result of their size and weight, these isolation systems are not ideal for all applications due to the additional weight and size they add to the overall design. There have been designs in the past that implemented open-loop or closed-loop cancellations to deal with systems that cannot use mechanical isolators. It is possible to cancel the vibration by measuring the vibrations and subtracting them from the phase noise, but such a system has disadvantages when it comes to vibration frequency and force changes. Both the vibration information and the phase noise measured by the feedback system are used in the feedback system. It uses these two inputs to compensate for the changes in signal frequency that occur because of vibration. During the design process, mechanical vibration dampeners were removed from the design to reduce their size and weight.[12]

Quartz crystal oscillators (QCSs) are the most used devices regarding time and frequency standards. Annually, 2 billion (2x109) quartz oscillators are manufactured, out of which there are two hundred and nine. These small devices are mostly built into wristwatches, clocks, electronic circuits, and other small devices. In addition, these electromagnets can also be found inside test and measurement equipment, such as counters, signal generators, and oscilloscopes, as well as in the core of every atomic oscillator. Crystal oscillators are electronic oscillators that use the mechanical resonance of a vibrating crystal of piezoelectric material. It creates an electrical signal with a constant frequency using the crystal's mechanical resonance. The signal will be created at a given frequency and converted into an electrical signal. For a long time, crystal oscillators have been regarded as the best frequency sources due to their excellent frequency stability, spectral purity, and low phase noise characteristics. Crystal oscillators can suffer from a loss of noise performance due to mechanical vibrations or other acceleration events in the environment in which they are to be used. It is widely accepted that virtually all microprocessors, microcontrollers, peripheral interface controllers (PICs), central processing units (CPUs), and CPUs use QCS as the frequency reference devices. Crystal oscillators are the most accurate and stable oscillators compared to resistor-capacitor oscillators in terms of accuracy and frequency stability. Since the effects of the oscillator over the vibration frequency range are more apparent with this overall vibration profile, it is commonly used to evaluate oscillators since there are a greater number of effects caused by the oscillator itself. [13]

In the frequency domain, the phase noise spectrum describes the stability of an oscillator as a function of its phase noise level. It can separate random noises (stochastic) from induced noises (deterministic) as well as repetitive noises (induced). It can be said that the frequency domain spectrum represents the spectral (frequency) content of the output of the oscillator over a certain range of frequencies. [14]

Several high-frequency applications can be accomplished using phase-locked loops (PLLs), from simple clock cleaning circuits to local oscillators (LOs), which are used in high-performance radio communication links, as well as ultra-fast switching frequency synthesizers in vector network analyzers (VNA).[15]

The phase frequency detector (PFD) is a PLL circuit's first and most essential element. A PFD is operated by comparing the phase of a waveform input to RFIN with a waveform output from RFIN that is the same frequency and phase. An example of this type of PLL is the ADF4002 PLL which blocks the diagram in Figure 3 (recommend the feedback divider N = 1 to configure it as a standalone PFD). Therefore, it can be combined with a voltage-controlled crystal oscillator (VCXO) and a narrow low-pass filter to clean up a noisy reference clock in the FREF port.

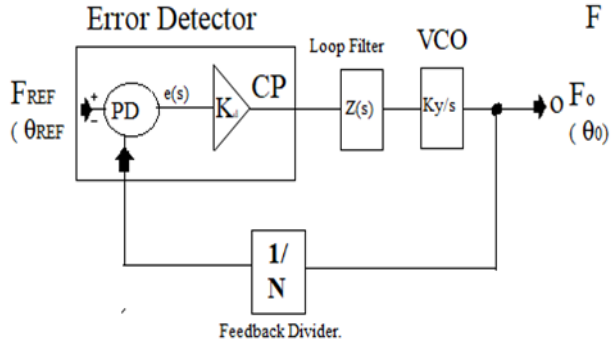

Figure 3. Basic PLL Configuration.

In its most basic configuration, a phase-locked loop compares the phase of a reference signal (FREF) to the phase of an adjustable feedback signal F0, as seen in Figure 3. Figure 4 shows a negative feedback control loop operating in the frequency domain. When the comparison is in a steady state, and the output frequency and phase are matched to the incoming frequency and phase of the error detector, then the PLL is locked.[15]

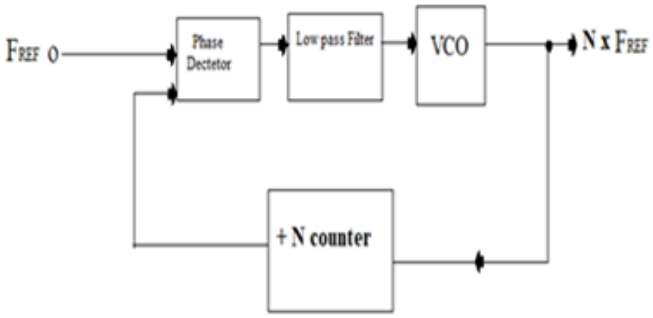

Figure 4. Basic PLL Configuration.

The Mechanical vibration effect on the oscillator's phase noise spectrum is derived and presented.[16]. The mechanical vibration frequency generates visible signals at the vibration frequency to the phase noise spectrum symmetrically to both sides around the oscillator's oscillation frequency. A 10 g force acceleration has been used in the phase noise spectrum example. [16]

3 VALIDATION MEASUREMENT SET-UP

The measurements were conducted in an EMC lab at the University of Oulu on the Linnanmaa campus. The over-the-air (OTA) measurements were performed with frequency extenders which were 48 cm apart from each other. It can be seen in the figure below that the measurement arrangement is photographed in Figure 5.

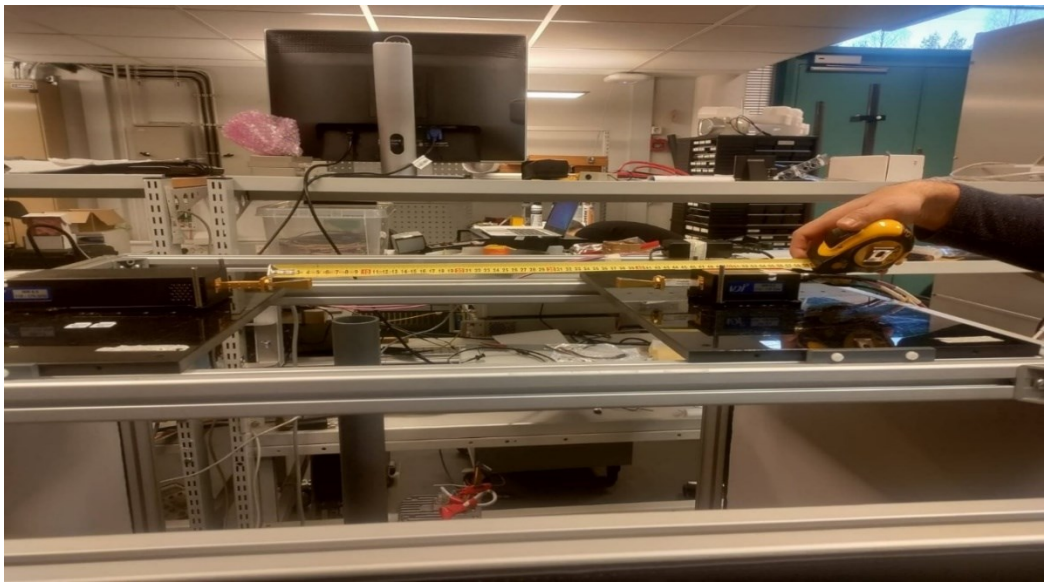

Figure 5. Frequency extenders in the over the air measurement arrangement.

3.1 Measurement setup with mechanical vibration

The mechanical vibration effect on the radio performance was measured with the Keysight vector network analyzer (VNA). The analysis is done based on the measured S-parameters of the OTA link. Mechanical vibrations of the measurement instruments, specifically frequency extenders, were measured with a G-force recorder mobile phone application installed into the mobile phone. The mechanical vibrations were measured by installing the mobile with an activated G-force meter on top of the frequency extender under measurement. The location of the mobile phone was changed between different measurement cases. As an example, the measurement case where the mobile phone is located over the receiver (Rx) extender is shown in Figure 6.

The mechanical vibrations were measured with a G-force Recorder application that uses an onboard accelerometer in the device for measurement. G-force meters can also measure the forward and lateral G forces and are used to calculate acceleration, velocity, and distance traveled using this data. The application is available in both Google and Apple stores. A front page of the G-force application Recorder is shown in Figure 7.

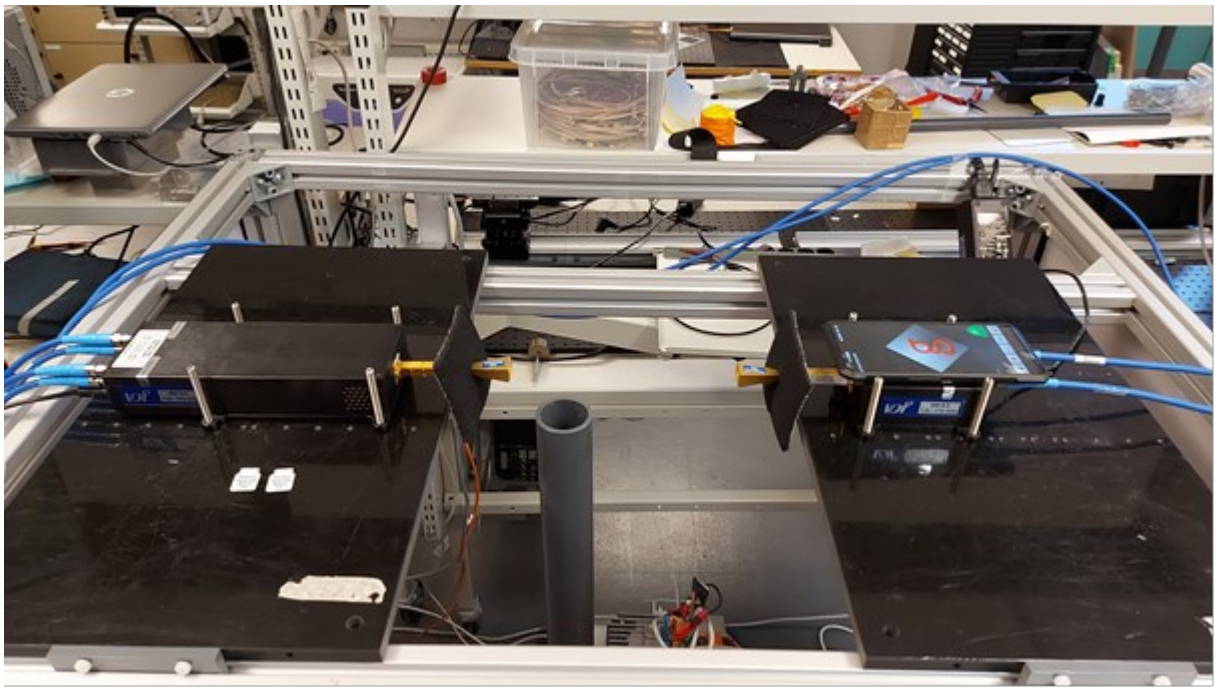

Figure 6. The measurement setup with G-force vibration measurement equipment on top of RX extender operating from 110 to 170 GHz.

Figure 7. G-force application Recorder

3.2 Network Analyzer for S-parameter measurement

The vector network analyzers are used to measure the components' scattering parameters. The parameters of the network. A wide variety of network analyzers is the most common use of two-port VNA. Which can measure two-port systems like amplifiers and filters, but network analyzers can also represent systems with any number of ports. Network analyzers are used in high-frequency ranges up to 67 GHz without frequency extenders. A network analyzer can also measure frequency ranges as low as 1 Hz using different types of equipment. [17]

Using the VNA is the best way to measure and characterize multi-port networks, for example, which consist of channels based on transmission lines/coaxial cables. Using the VNA, it is possible to characterize passive and active devices operating at high frequencies in their linear mode of operation by measuring their scattering network parameters, also called S-parameters. [17]. In our measurement, we have used a VNA from Keysight, which can be seen in picture 8 below.

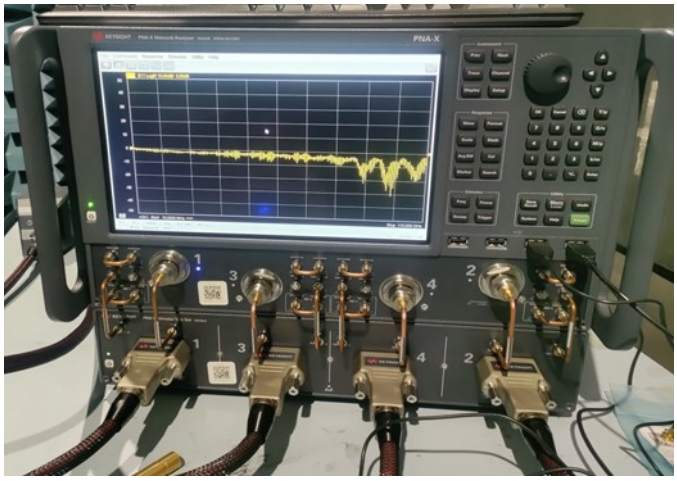

Figure 8. Keysight's Network analyzer

To measure noise parameters and nonlinear characteristics on top of S-parameters in the VNA, modern VNAs are frequently updated and extended within hardware options. In this way, the VNA can perform multiple measurements in a single setup, resulting in time savings. The VNA has many benefits, including its accuracy and high dynamic range. The calibration program allows the probe and the adapter effects on the measurement results to be compensated. Because the measurement results analysis is usually done in the frequency domain, it is convenient to measure and work with the frequency parameters. The VNA can be used to measure time-domain effects and transitioning from a frequency domain into a time domain can either be conducted directly in a VNA using the inverse Fourier transform or, after the fact using analysis software in post-processing. Figure 9 shows the measurement results of the VNA used during the time domain measurement. During a VNA measurement, the measuring frequency range and the number of points selected within a given frequency band. [17]

The scattering parameters (S-parameters) of a circuit enable an analysis of the stability of the circuit, the input and output reflection coefficients, and the power gains. The S-parameters include amplitudes and their phases of the relationships between different ports.

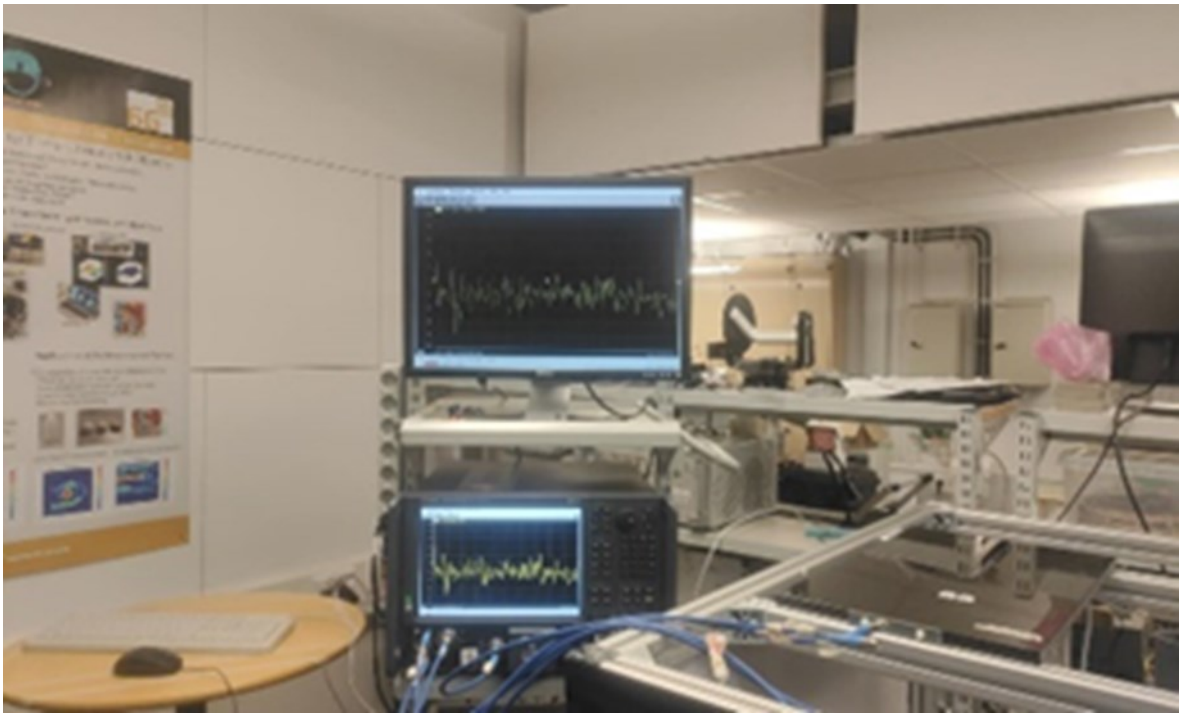

Figure 9. The measurement result display of VNA with time domain measurement.

3.3 Frequency extenders

The frequency extenders are used to extend the frequency band for the measurement equipment to measure the frequencies above the original maximum frequency. Virginia Diodes Inc. (VDI) is the manufacturer of the frequency extenders used in these measurements. They offer banded waveguide extenders, calibration kits for S-parameter measurements, and calibration kits for extension modules. Two different calibration techniques will be offered depending on the frequency at which the system will be operated. In our measurement case, the frequency converters WR6.5 are used, which extends the measurement range to the frequency band from 110 GHz to 170 GHz from 50 GHz to 1,500 GHz. Figure 10 illustrates a full transceiver (TX/RX) module that can be used as an example. The TRX module enables S-parameter measurement of reflected and transmitted parameters such as S11 and S21. A photograph RX extender is shown in figure 11. The power level that PM5 can measure is up to 1000mW. Since the TRX extender is a fixed output power device, micrometer-driven attenuators can adjust the attenuation by 0-30dB, thus controlling the TX power level 30 dB down from the maximum. [19]

Figure 10. TRX frequency extender from VDI for 300 GHz application.

Figure 11. RX extender from VDI for 300 GHz application.

3.3.1 *Used Frequency Extender connections*

To function properly, several cable connections are required between the frequency extenders and VNA. We have used Keysight PNA (performance network analyzer) as VNA in our measurements. The TRX frequency extender is connected to PNA following: [18], [19]

- VNA Port 1→TRX extender port RF
- VNA Port 3 → TRX extender port LO
- VNA RCVR A IN → TRX extender port M
- VNA RCVR R1 IN → TRX extender port R

The photographs of the front-panel of the PNA and TRX extender connection ports are shown in Figure 12.

Figure 12. Front panel of PNA and TRX extender connection ports[18]

The photograph of the complete cabling of the TRX module with PNA analyzer is shown in Figure 13. [18],[19]

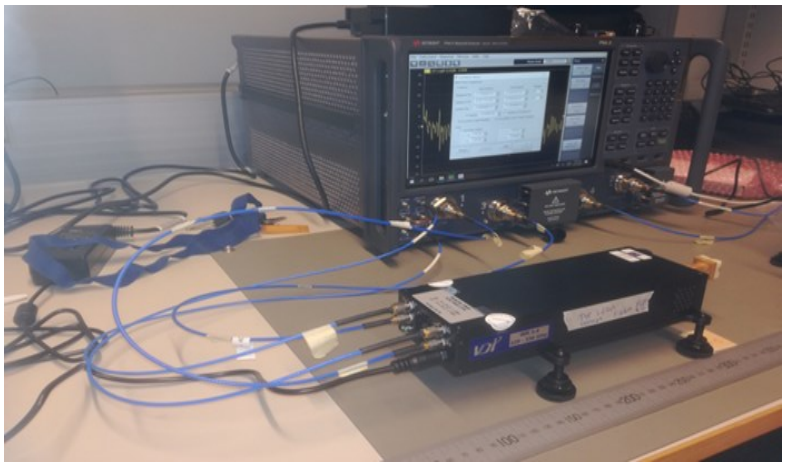

Figure 13. PNA-X connections to TRX- extender port. [18]

The RX frequency extender connection to the PNA is following: [18], [19]

- VNA Port 2 → TRX extender port M
- VNA Port 4 → TRX extender port LO

The photograph of the RX extender connection ports is shown in Figure 14.

Figure 14. RX extender connection ports to PNA-X (Network Analyzer).

3.4 Calibration

A vector network analyzer can make precise network measurements by correcting for cable characteristics and systematic errors within the instrument. A term called calibration is commonly used to describe the error correction process. However, it is sometimes referred to as user calibration to indicate a difference from periodic calibrations performed by manufacturers. In the measurement calibration, known standards are measured to compensate for systematic errors by using the known standards as references. [18]

3.4.1 *Calibration Kit*

Equipment typically supplied for Type A and Type B TRL calibration is shown in Figures 14 and 15. This kit's label (above) is modified to reflect the specific contents of the calibration kit.

Figure 14. Calibration Kit for WR 3.4

Figure 15. Content inside the box

It is possible to calibrate network analyzers using waveguide calibration standards included in the calibration kit. As part of this kit, we have received fixed terminations, open circuits, short circuits, broadband loads, adapters, and broadband loads. It is specified that this the WR6.5 calibration kit is specified and capable of measuring frequencies between 110 and 170 GHz. [18]

Figure 16. Short

Figure 17. 50 Ohm load

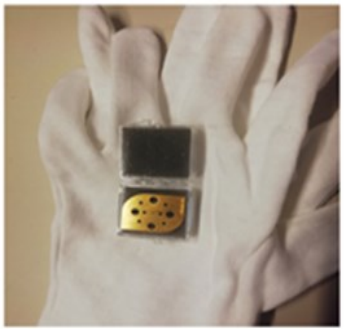

Figure 18. Quarter wave delay shim

3.4.1 *Calibration, Extenders back-to-back*

In the frequency extender calibration, a partial 2-port calibration can be done since S12 and S22 cannot be measured due to the lack of a second transmitter inside the RX extender. During full 2-port calibration, as illustrated in Figure 19, the calibration data are calculated to determine the accuracy of the calibration system by connecting an OPEN standard, a LOAD standard, or a SHORT standard to two desired waveguide test ports. As a result of this calibration, directivity error, source match error, frequency response reflection tracking error, frequency response transmission tracking error, and crosstalk are effectively eliminated.[20]

A photograph of the configuration where extenders are back-to-back is shown in Figure 20. The through (thru) configuration is shown in the configuration in Figure 20.

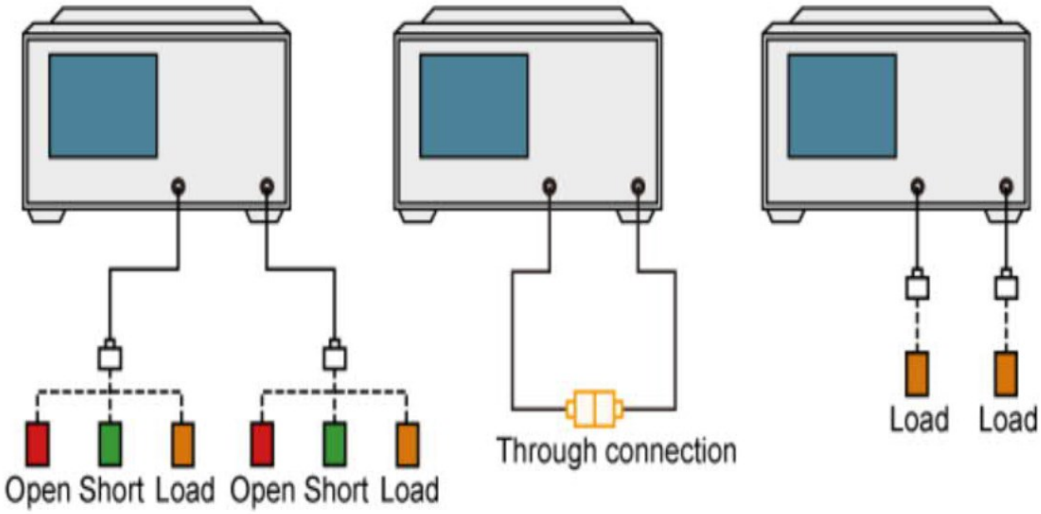

Figure 19. Connecting standards in full 2-port calibration

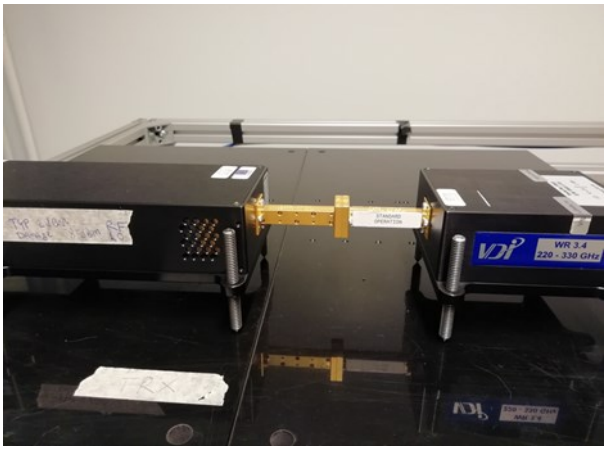

Figure 20. 220-330 extenders connected back-to-back configuration. [18]

3.4.1 *Calibration with Quarter wave Offset shim*

The quarter wave-length shim calibration was used when extenders were connected back-to-back. The calibration with quarter wave-length shim is available from WR19 (40 – 60 GHz) through WR3.4 (110-170 GHz). Alternatively, the calibration method SOLT (Short-Open-Load Through) is available from WR28 (26.5-40 GHz) through WR1.0 (750-1000 GHz). Two VDI style reports are available in calibration kits in the current version: Type A (legacy style, round) and Type B (current style, rectangle). Standard calibrations support QW (Quarter Wave Delay Short) and QD (Quarter Wave Delay Short) methods. Both short + ¼ offset shim and load (50 ohms) + and ¼ offset shim are connected to the RF port of the extender in turn to obtain needed calibration coefficients. Additionally, direct back-to-back measurement is performed. A photograph of short calibration and ¼ offset shim standards as standalone are shown in Figure 21. The photograph of the connected load and ¼ offset shim to the waveguide output at the TRX extender is shown in Figure 22. The rectangle-style shim has been used for the calibration, as shown in Figures 21 and 22. [20]

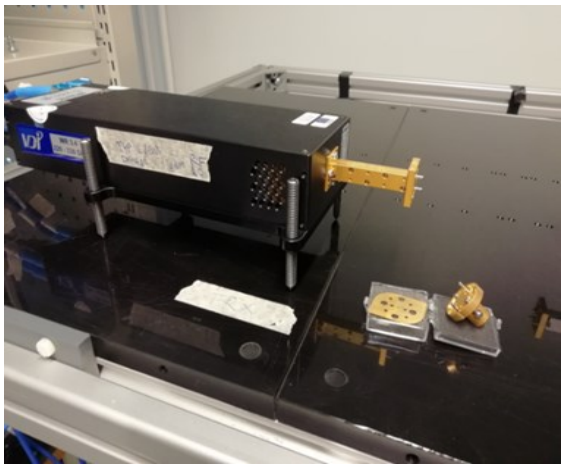

Figure 21. Short and ¼ offset shim calibration standards.

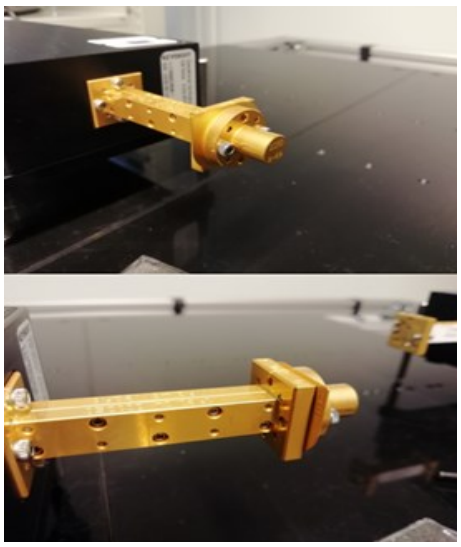

Figure 22. Load and ¼ offset shim connected to extender's waveguide output.

3.4.2 *Enhanced Response Calibration*

When the enhanced response calibration is used, the measurements are done in one direction. In such measurements, calibration standards open, short, or load are connected to the extender's output port. When the calibration is done in this manner, it will eliminate all directivity errors, crosstalk, source matching errors, frequency response reflection tracking errors, and frequency response transmission tracking errors that may be caused by the test setup in a transmission or reflection test that makes use of those ports. [19]

As a result of this calibration, extenders can be used back-to-back or over the air when connected. In a flush-through calibration method, the thru standard (back-to-back) is connected between two RF waveguide ports, which means that the thru standard has zero length for any process: no delay, loss, no capacitance, and no inductance. [18],[19]

4 MEASUREMENT RESULTS OF VIBRATION TESTS WITH 140 GHZ SIGNAL

Mechanical vibration tests have been done in EMC laboratory at Oulu university with over-the-air link which performance was measured with VNA. Several mechanical vibration tests were conducted for the thesis for example: back-to-back, knocking of the table at the receiver extender side as well at the transmitter side. Different kind of experiment cases were done by adjusting and leveling the extenders with the adjustment screws when the over-the-air link was activated. Additionally, knocking tests were conducted when the extenders were connected directly back-to-back configuration.

The measurement data analysis was done with readymade Matlab-software which was coded by Dr. Nuutti Tervo, some updates done by Dr. Marko E. Leinonen.

4.1 Vibration with back-to-back extenders

First the vibration tests were done by vibrating back-to-back extenders as shown in Figure 20. The G-force vibration measurement results of the back-to-back are shown in Figure 23. The vibration measurement was done over 34 seconds time-period. First there was silent period of 4 second which is visible from the figure 23. The end of the silent period is marked with a marker tip on X: 4379. After silent period, now we can see the G-force measurement results changes from 1018 and the G-force changes to 1280 mG or 1.28 G as shown at Y-axis during the vibration period.

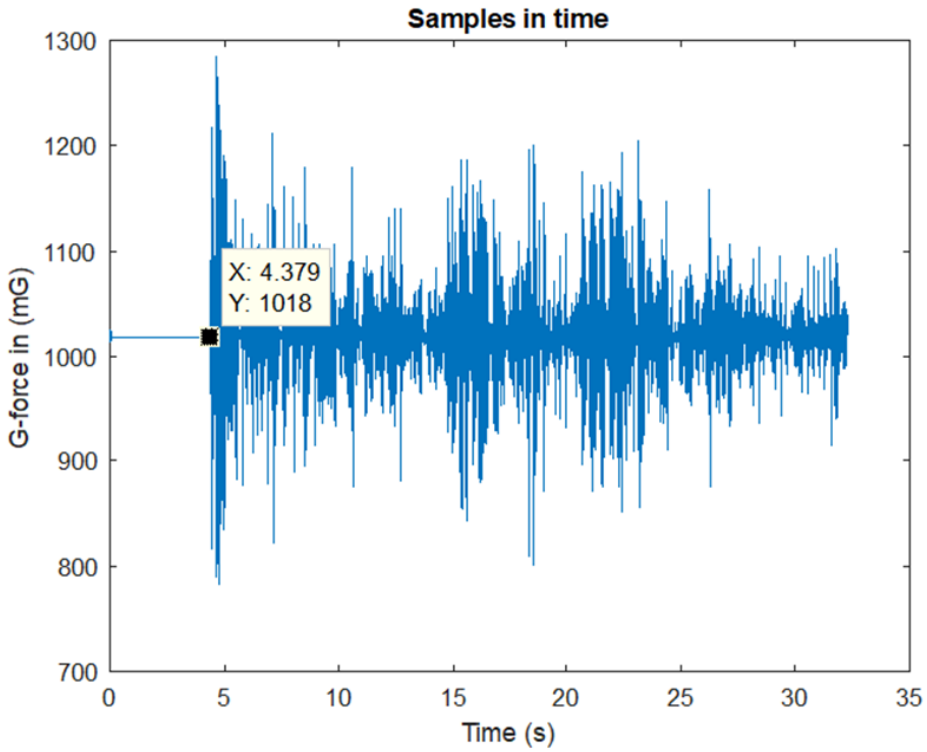

Figure 23. Mechanical vibration results, Vibration with back-to-back extenders

The effect of mechanical vibration can be also seen from the in S11 scattering parameter of the air link phase change response which are shown in Figure 24. The phase change of the vibration measurement is shown over 2 seconds time-period in which is only faction of total measurement time. First there was silent period of 2.4 second which is visible from the figure 24. The silent periods of mechanical and phase measurements are thus aligned. The end of the silent period is marked with a marker tip on X: 2.599. After silent period, now we can see the phase measurement results changes from 73.25 degrees up to 76.5 degrees at Y-axis during the vibration.

.

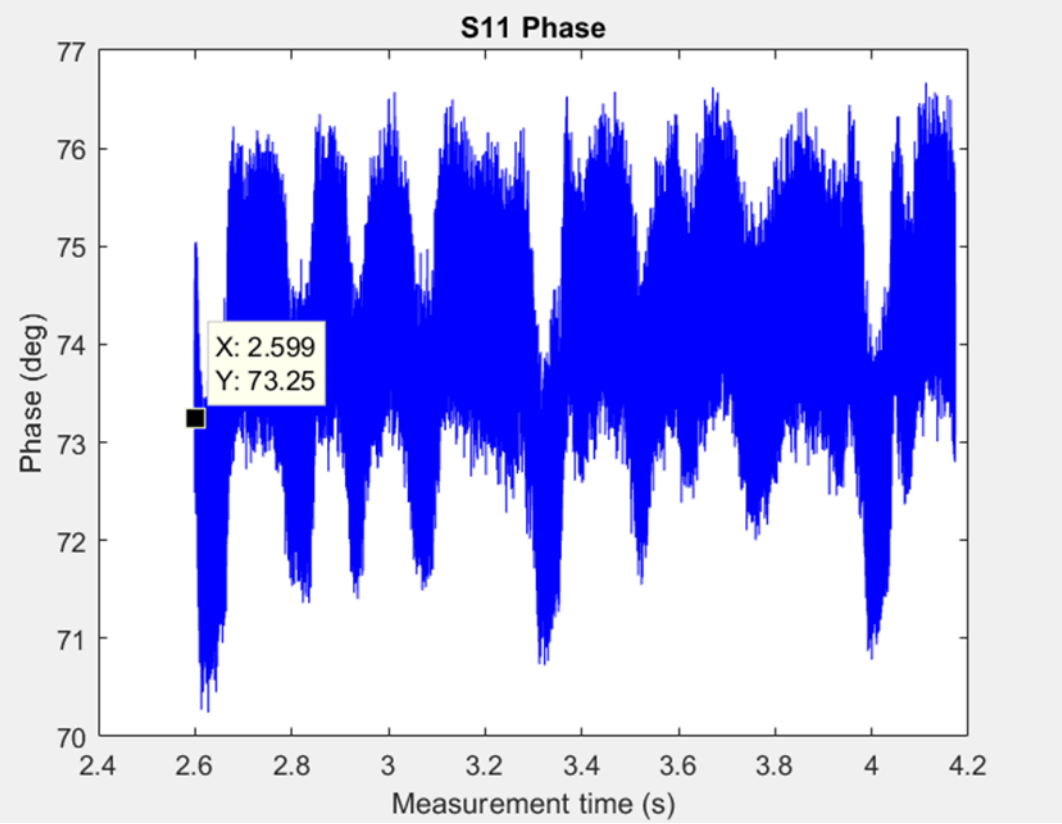

Figure 24. Over-the-air link S11 phase change due to mechanical vibration, back-to-back extenders; zoomed in the vibration time.

The effect of mechanical vibration can be also seen from over the in S21parameter of the air link phase change response which are shown in Figure 25. The phase change of the vibration measurement is shown over 4.2 second time-period in Figure 25. First there was silent period of 2.6 second which is visible from the figure 25. The end of the silent period is marked with a marker tip on X: 2.599. After silent period, now we can see the S21 phase measurement results changes from -156.8 degrees between -159 and -154 degrees at Y-axis during the vibration.

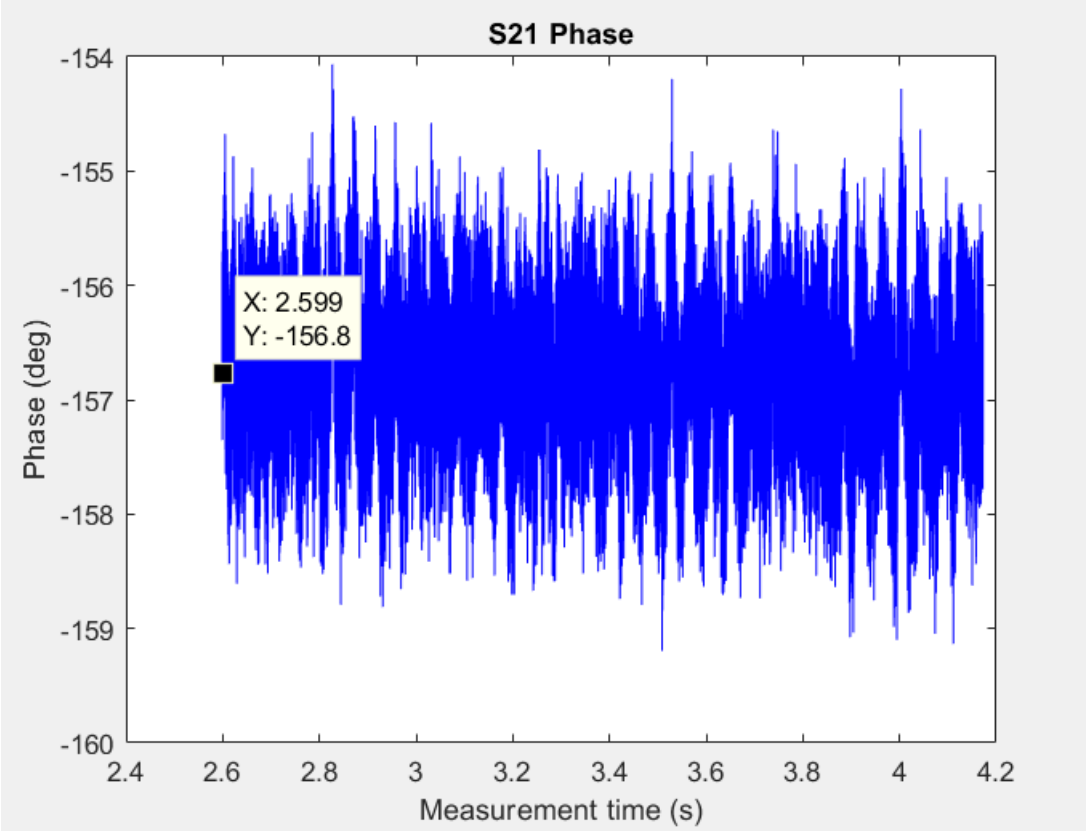

Figure 25. Over-the-air link S21 phase change due to mechanical vibration, back-to-back extenders; zoomed in the vibration time.

4.2 Vibration at receiver side with OTA link

After conducted tests OTA tests were done. First the vibration tests were done at receiver side by knocking the table at that side. The G-force vibration measurement results of the OTA link direction are shown in Figure 26. The vibration measurement was done over 21 second time-period. First there was silent period of four second which is visible from the figure 26. The end of the silent period is marked with a marker tip on X: 3.943. After silent period, the mechanical vibration was experienced from 3.943 to 5.384 second. Now we can see the G-force measurement results changes during period of 3.943 to 5.384 seconds. The G-force at silent period was 1.021 G and 1.017 G. During the vibration period of 3.943 to 5.384 seconds the G-force chances to 1.062 G at Y-axis during the vibration.

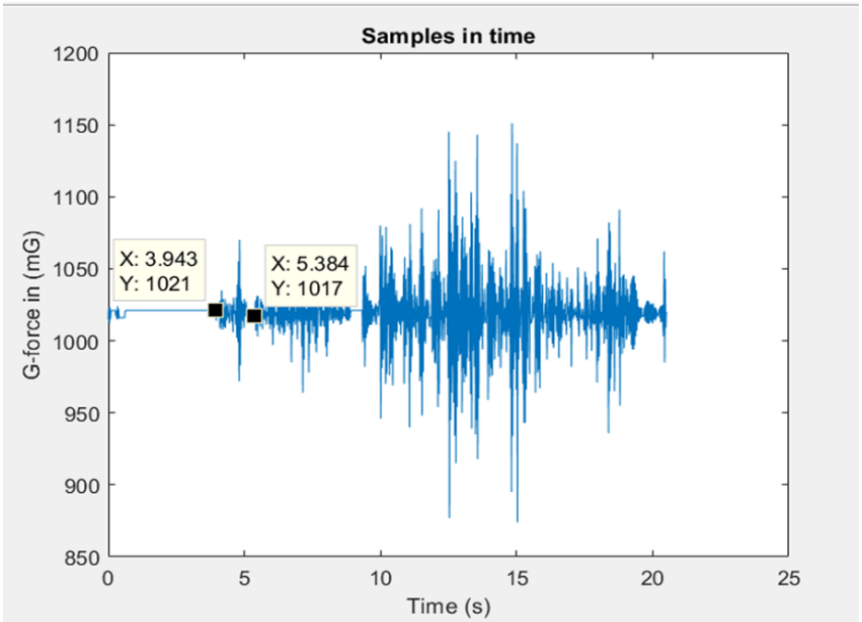

Figure 26. Mechanical vibration results, when knocking done at receiver side.

The effect of mechanical vibration can be also seen from over the in S21 air link phase change response which are shown in Figure 27. We can see change in phase more than 81.4 degrees in time period of 2.731 to 4.171 seconds. The time instance of 2.7131 seconds in S21 measurement corresponds time instance of 3.949 seconds in mechanical vibration measurement. Similarly phase change can be seen at 10 seconds time instance which corresponds vibration staring at 12 seconds in the Figure 27. At that time the S21 phase changes 114 degrees.

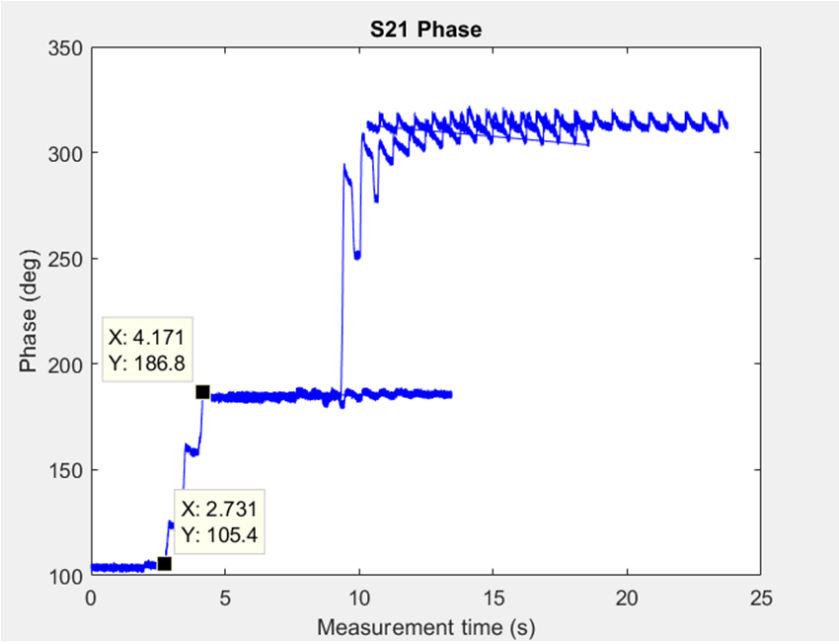

Figure 27. Over-the-air link S21 phase change due to mechanical vibration, when knocking done at receiver side; full experiment time.

The effect of mechanical vibration can be also seen from over the in S21 air link phase change response which are shown in Figure 28. which is zoomed version of Figure 27. We can see change better the shape of the phase changes. Its look like a stairs case.

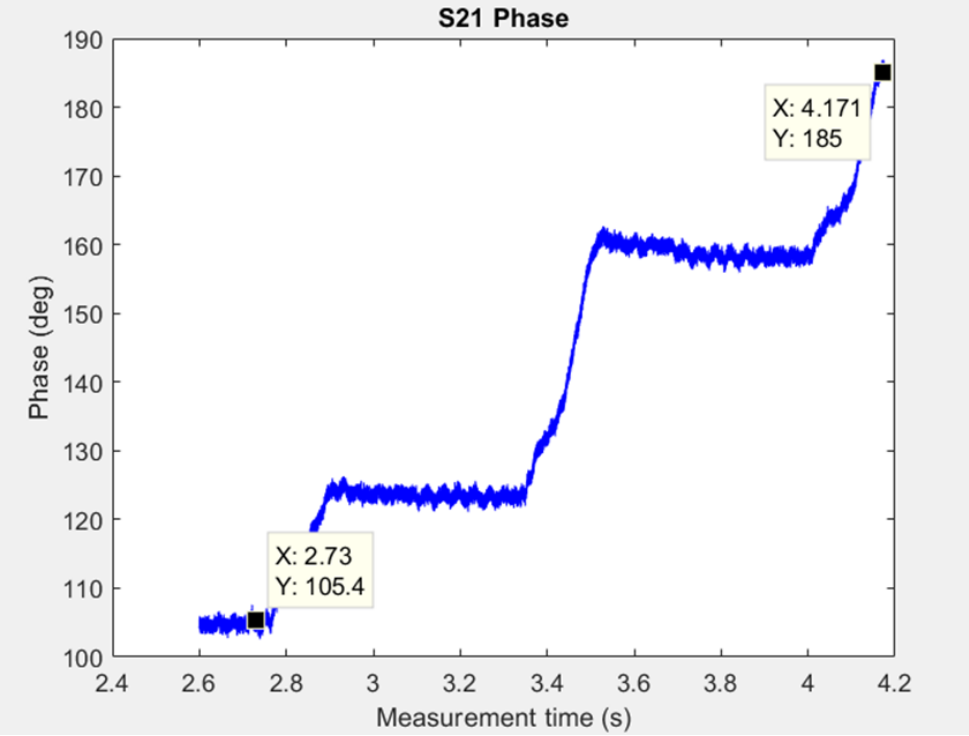

Figure 28. Over-the-air link S21 phase change due to mechanical vibration, when knocking done at receiver side; zoomed in to first vibration time.

The mechanical vibration can be also seen from over the in S11 air link phase change response which is shown in Figure 29. The S11 phase changes more than 40 degrees between time instances of 2.73 to 4.171 seconds. Similarly phase change can be seen at 2.7 seconds time which corresponds vibration at 4.1 second time instance in the Figure 29. The magnitude of phase change in S11 is a half of the S21 phase change in the analysed time interval.

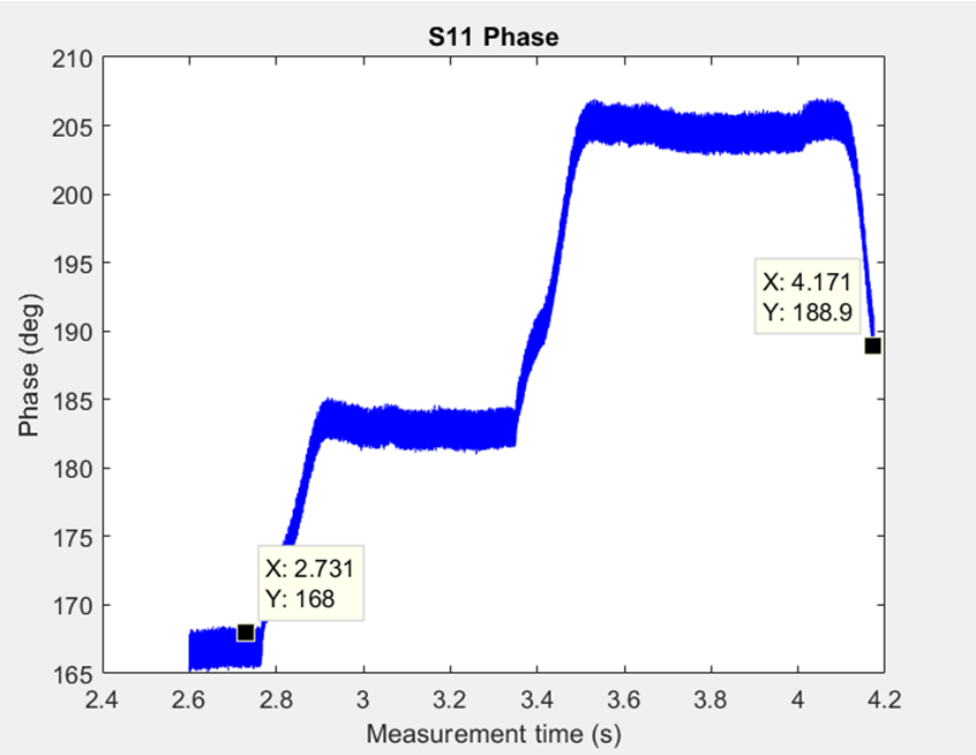

Figure 29. Over-the-air link S11 phase change due to mechanical vibration, when knocking done at receiver side; zoomed in to first vibration time.

4.3 Fast Vibration at transmitter side with OTA link

Mechanical vibration has been done in transmitter side in this vibration case. The G-force vibration measurement results of the (fast knocking) are shown in Figure 30. The vibration measurement was done over 28 second time-period. First there was silent period of eight seconds which is visible from the Figure 30. It is marked with marker tip on X: 8.611.

Mechanical vibration experience starts at time of 8.611 seconds and the largest amplitude is at 9.332 seconds. The G-force measurement results change from 1.020 G up to 1.369 G which can be read from Y-axis.

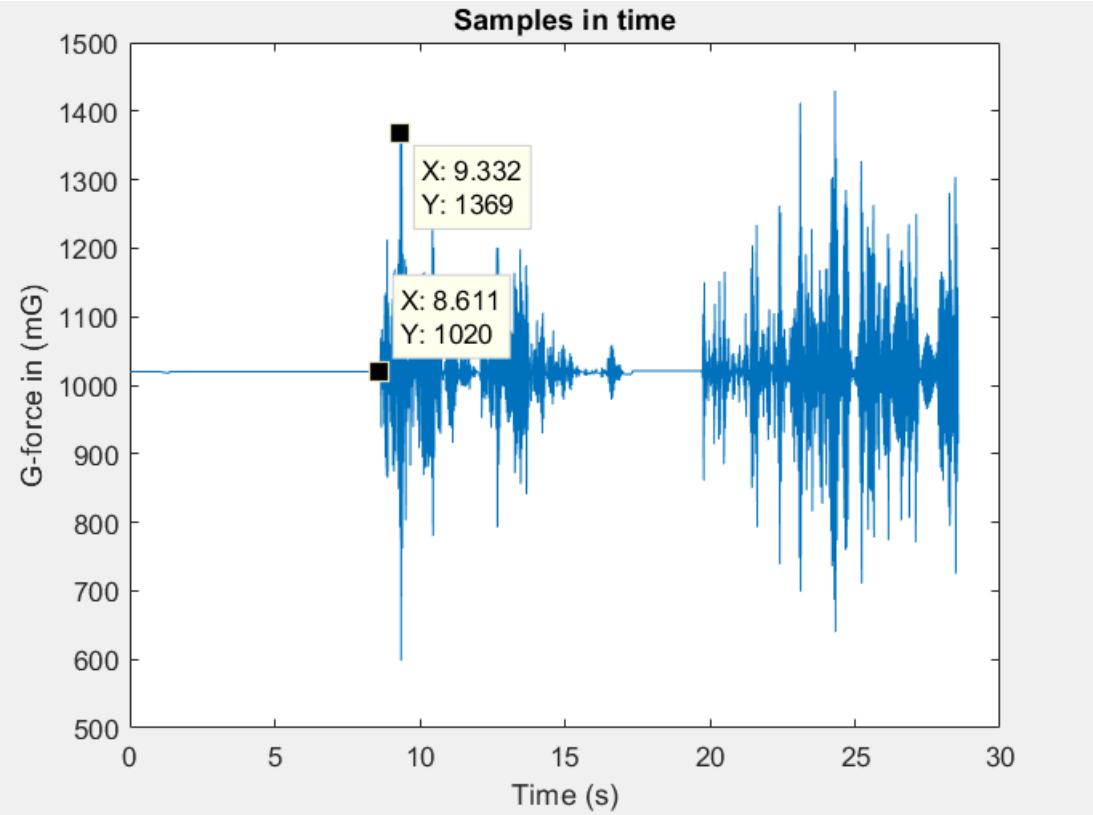

Figure 30. Mechanical vibrations measurement when fast knocking was done at transmitter side.

The effect of mechanical vibration changes the phase response of S11 in the over air link which is shown in Figure 31. The initial value of the phase of S11 was 177.4 degrees in time instance of 2.599 seconds when the measurement stared. The starting point of the S11 measurement (2.599 seconds) corresponds the time instance of 8.611 seconds in the Figure 31. The phase of S11 changes only within 10 degrees during the measurement window.

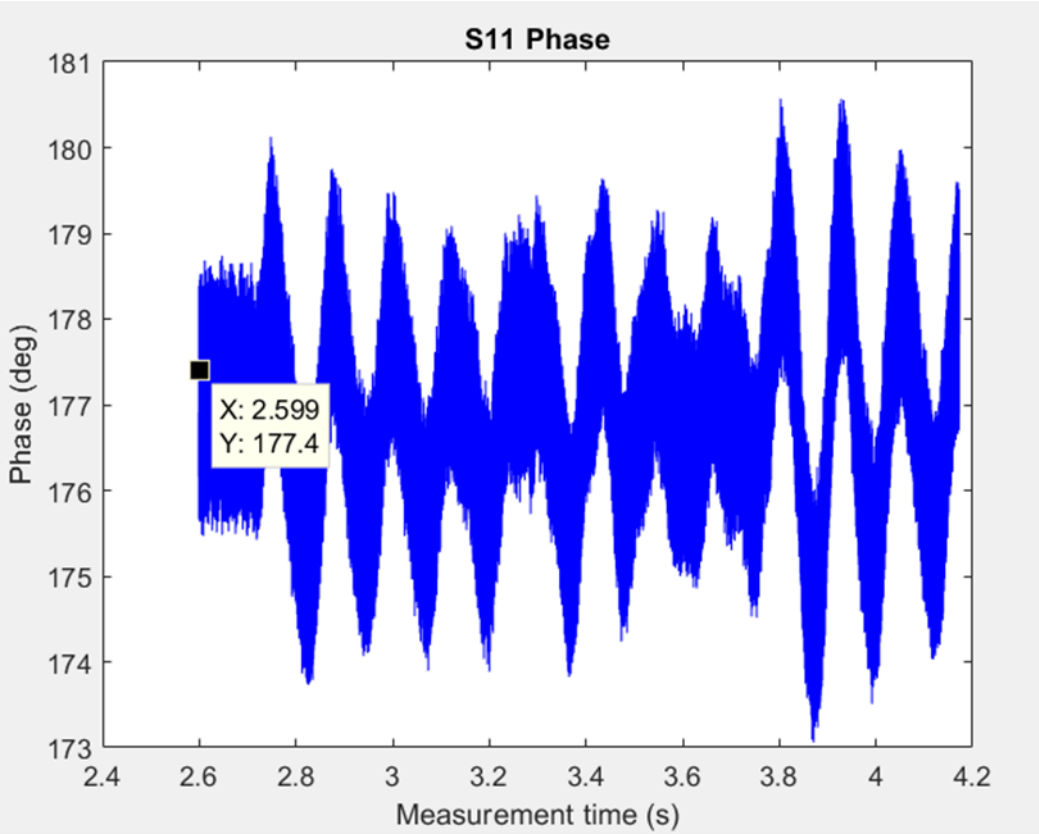

Figure 31. Mechanical vibrations measurement S11 phase change was done when fast knocking was done at transmitter side; zoomed in to fast knocking vibration time.

The effect of mechanical vibration can be also seen from over the in S21 air link phase change response which are shown in Figure 32. We can see change from the phase of 132.9 degrees in time instance of 2.599 seconds. First there was silent period of 2.5 second which is visible from the figure. Similarly phase change can be seen at that time which corresponds 4.2 second vibration in the Figure 32 and a similar Legacy phase change is which is visible in Figure 29. Same effect of mechanical vibration can be also seen from over the air link phase change response which are shown in Figure 32. We can see change in phase the vibration measurement was done over 4.2 s time-period. The end of the silent period is marked with a marker tip on X: 2.599.

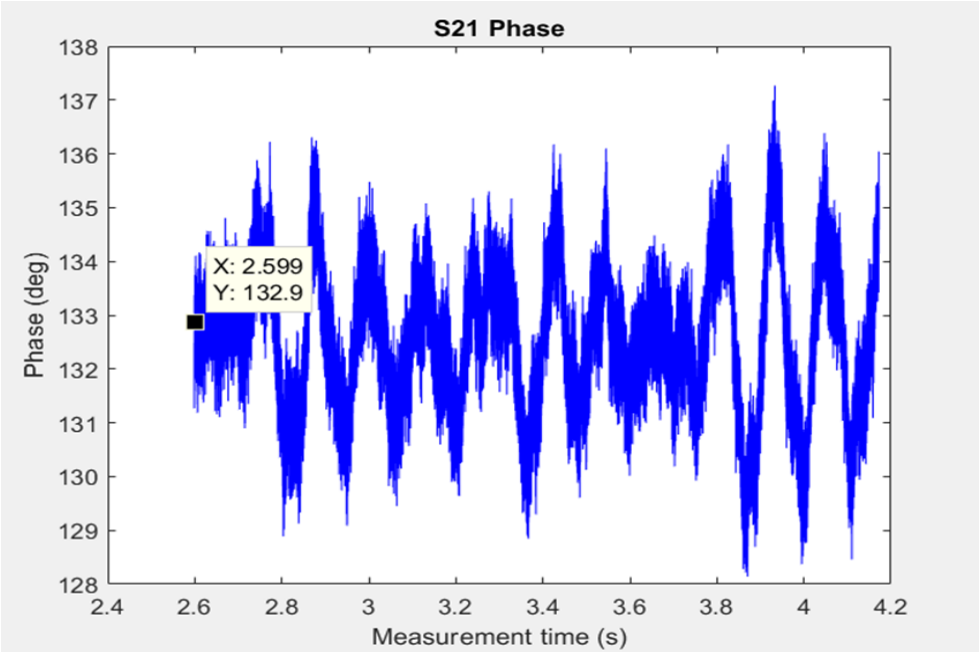

Figure 32. Mechanical vibrations measurement S21 phase change was done when fast knocking was done at transmitter side; zoomed in to fast knocking vibration time.

4.4 Higher OTA link level vibration at transmitter side with OTA link

The OTA link level was changed by tightening the screws attached to the extenders, and thus the level of the link changed. The used screws are shown in Figure 33.

Same effect of mechanical vibration with tighter screws conditions can be seen from over the air S21 link phase change response which is shown in Figure 33. First there was silent period of 4 second which is visible from the figure 33. The end of the silent period is marked with a marker tip on X: 4328, After silent period, now we can see the G-force measurement results changes from 4328 and the force changes from 1026 G at Y-axis during the vibration.

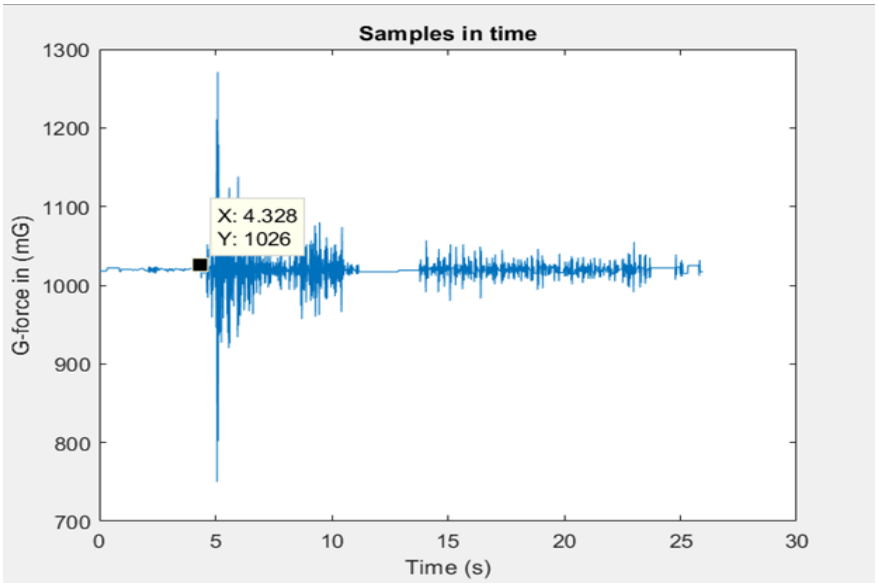

Figure 33. Mechanical vibrations measurement when transmitter side screws were tightened, and the OTA link level raised.

The mechanical vibration affects to the over the in S21 air link phase response which is shown in Figure 34. First there was silent period of 2.5 second which is visible from the Figure 34. The end of the silent period is marked with a marker tip on X: 2.734. After silent period, now we can see the G-force measurement results changes from -166.4 degrees to step manner.

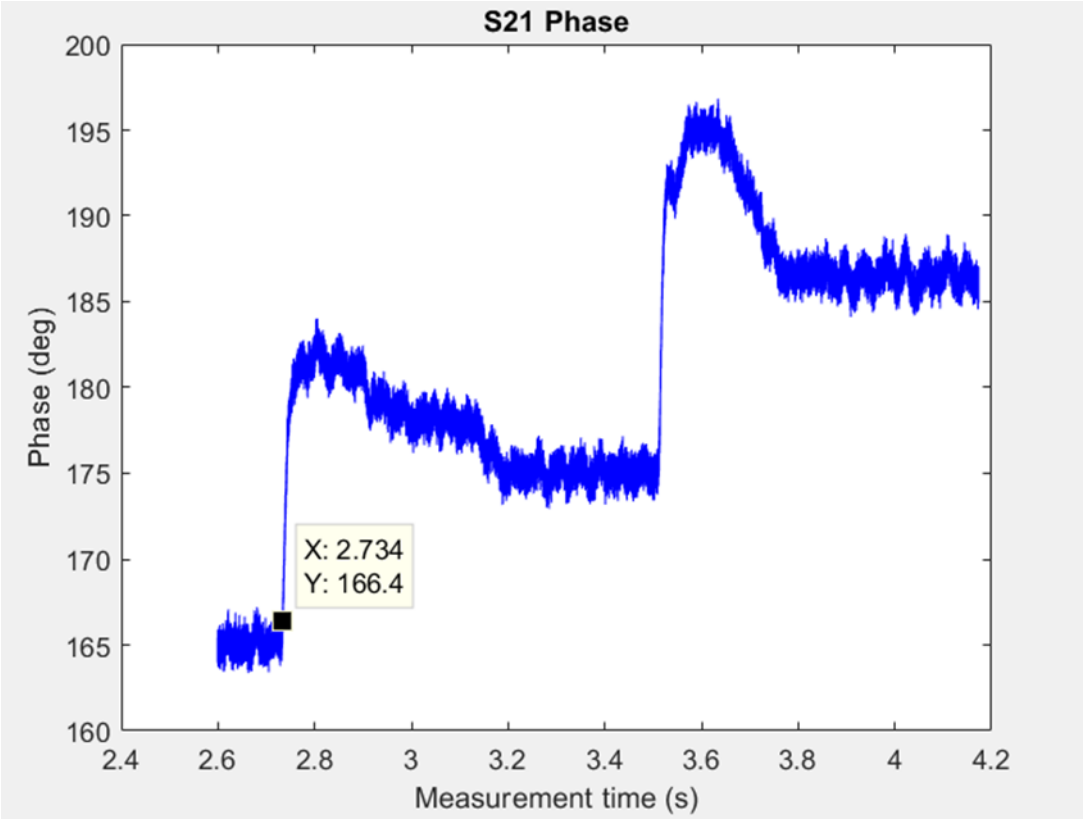

Figure 34. Over the air link S21 phase measurement when transmitter side screws were tightened.

The effect of mechanical vibrations in the measurement of S21 amplitude when transmitter side screws were tightened, is shown in Figure 35. First there was silent period of 2.8 seconds, and the end of the silent period is marked with a marker tip on X: 2.777. After silent period, now we can see the S21 measurement results changes from -24.65 dB by 0.3 dB as a step manner. This indicates clearly that phase measurement is more sensitive to mechanical vibration compared to amplitude measurement based on results from Figures 34 and 35.

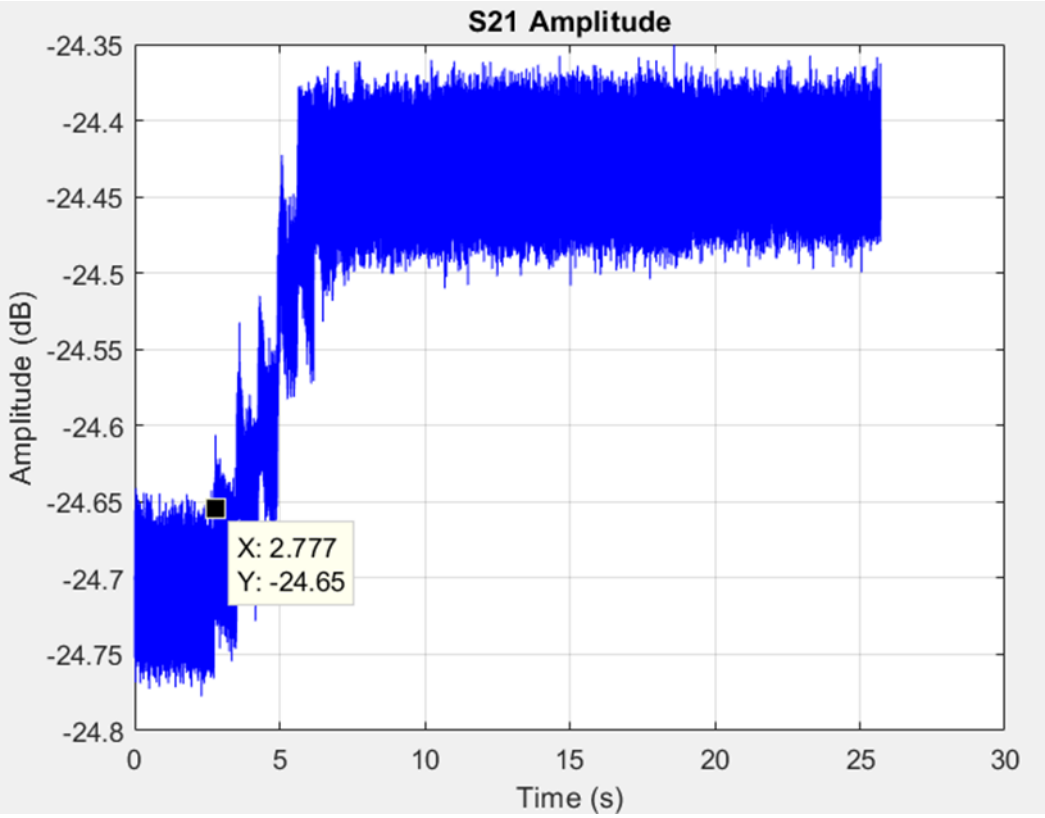

Figure 35. Over the air link S21 amplitude measurement when transmitter side screws were tightened.

Mechanical vibrations measurement S11 amplitude measurement when transmitter side screws were tightened are shown in Figure 36. Only transmitter side reflection measurement was done due to limitations of the extenders. The time instance of 2.727 seconds in S11 measurement corresponds time instance of 3.949 seconds in mechanical vibration measurement. At that time the amplitude changes from -15.87 dB down to -31.7 dB.

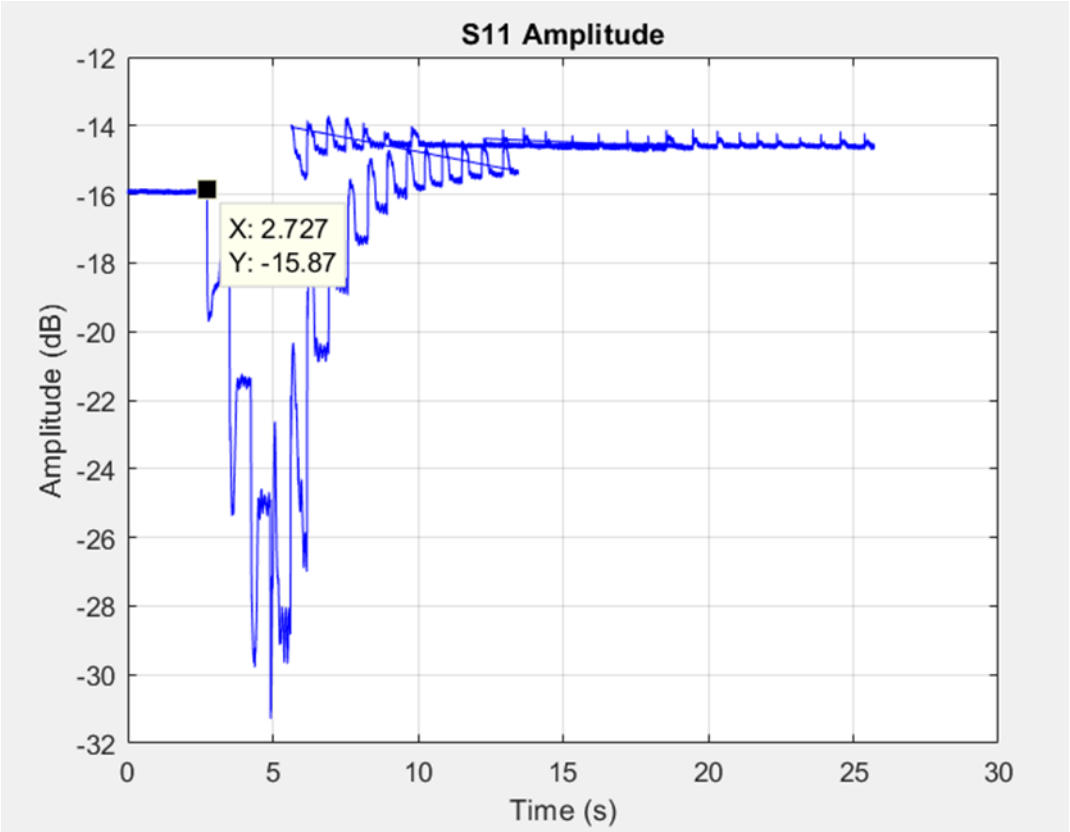

Figure 36. Over the air link S11 amplitude measurement when transmitter side screws were tightened.

The effect of mechanical vibrations OTA link S11 phase measurement when transmitter side screws were tightened is shown in Figure 37. First there was silent period which is visible from the Figure 37. The end of the silent period is marked with a marker tip on X: 2.735. After silent period, the phase of S11 measurement results changes from an average of -152 to -145 degrees as step manner when the vibration starts.

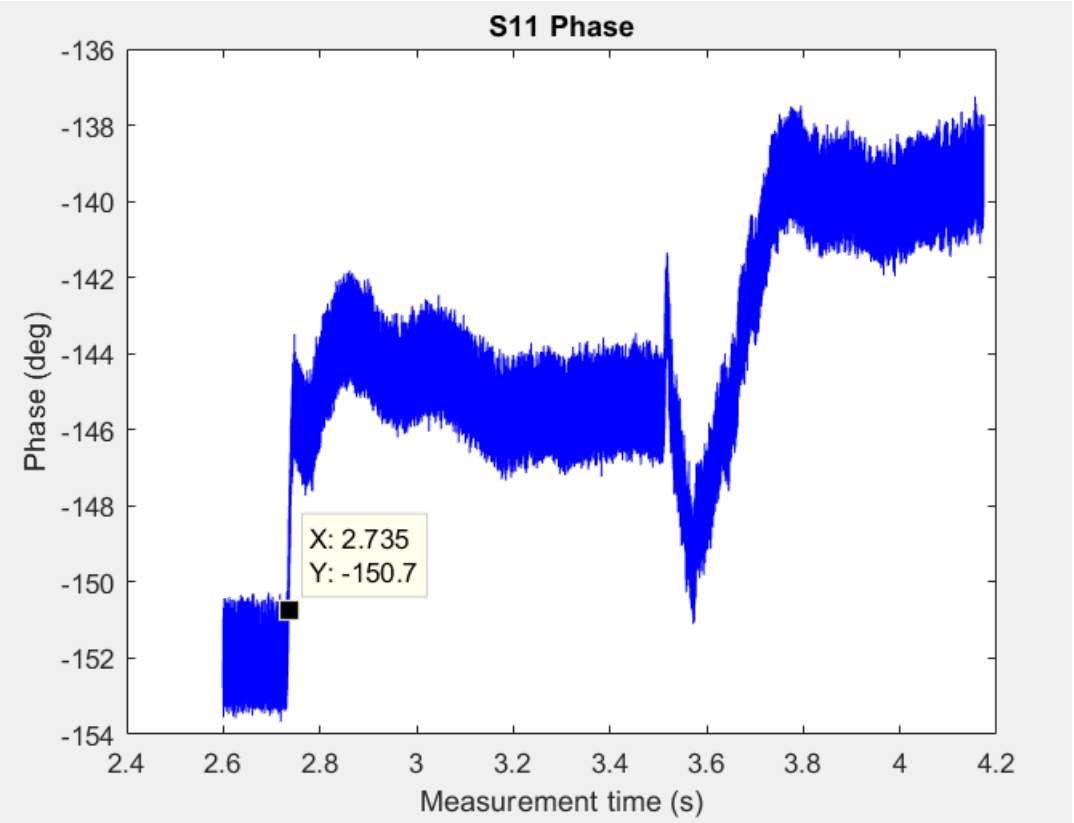

Figure 37. Over the air S11 phase measurement when transmitter side screws were tightened.

5 DISCUSSION

The thesis concentrated on mechanical vibrations and effect of those to OTA radio link parameters based on the practical measurements. The measurement results show clearly that mechanical vibrations influence the radio signal phase and thus it needs to be considered in the future development of 6G. Some practical measurements have been performed to verify the effects of mechanical vibration on wireless link performance.

The actual measurements were conducted in an EMC lab University of Oulu on the Linnanmaa campus. Mechanical vibration tests had been done in laboratory environment with an over-the-air link running 140 GHz and which performance was measured with the VNA. Several mechanical vibration tests were conducted for the thesis for example: back-to-back, knocking of the table at the receiver extender side as well at the transmitter side. The frequency extenders have been used to extend the performance of the RF measurement equipment over the original frequency range of 67 GHz to 140 GHz. The measurements were done with two different types of extender modules: one for TX and one for RX. Each module was attached a horn antenna supporting the full operational band of 110 to 170 GHz.

First knocking tests were conducted when the extenders were connected directly back-to-back configuration. After those, different kind of experiment cases were done by adjusting and leveling the extenders with the adjustment screws when the over-the-air link was activated.

We conducted the OTA measurements with the help of frequency extenders. During this experiment, a VNA was used to measure the reflected signal strength over a radio propagation path to measure the reflected signal strength. There has been a calibration of the vector network analyzer measurements to correct for cable characteristics and systematic errors in the instrument as well. As part of the calibration process, 50 ohms, open and short known standards were calibrated, and then the systematic errors were corrected based on those standards. The OTA measurement has been done with G-force measurement and vector signal analyzer measurements of the S-parameters of the wireless link. Based on the measurements, the phase response of the measured S-parameters is more sensitive to the vibration than the amplitude. The mechanical vibration has been measured with a mobile phone application which detects the changes, vibrations, and location changes of the mobile phone when it was placed over the frequency extender. The used mobile phone application was the G-force meter, which is freely available from application stores. The mechanical vibrations were measured with mobile terminal G-force measurement application which was easy to use.

The measurement data analysis was done with readymade Matlab-software which was coded by Dr. Nuutti Tervo, some updates done by Dr. Marko E. Leinonen. The measured S-parameters including amplitudes and phases of S11, and S21 air link phase were analyzed with the Matlab software which was provided for the purpose. It should be noted that only a fraction of the measurement results was presented in the thesis.

Based on the above scenarios, one could conclude that an assessment process can be effective in providing the results we need. To achieve the desired results. It can be concluded from the results of the experiment that it was successfully done.

6 SUMMARY

Mechanical vibrations will affect the performance of the wireless link especially with coming 6G systems, there will be a significant difference in the frequency at which these networks operate when compared to the current 5G networks. The mechanical vibrations affect the frequency generation circuitries of the radio equipment and thus the performance of the radio link.

The amount of the mechanical vibration to the radio or any equipment has been standardized and a short summary of related standards has been given in the thesis.

Over-the-air radio link measurements were performed when mechanical vibrations were done by knocking the table and the frequency extenders. The measurements showed clear effect of mechanical vibration to the phase response of the radio link when it was measured with network analyzer in time domain.

The practical OTA measurement with mechanical vibrations has been done with vector signal analyzer measurements of the S-parameters of the wireless link and G-force application measurement. Based on the measurements, the phase response of the measured S-parameters is more sensitive to the vibration than the amplitude. The measured S-parameters S11 and S21 were analyzed with Matlab software which was provided for the purpose. The measured S-parameters and vibration results have been time synchronized in the Matlab result post-processing.

The measurement results show clearly that mechanical vibrations influence the radio signal phase and thus it needs to be considered in the future development of 6G.

7 REFERENCES

[1] 5G is the fifth-generation network. https://en.wikipedia.org/wiki/5G

[2] Huawei's David Wang: Driving Industry Development with F5.5G https://telecoms.com/intelligence/huaweis-david-wang-driving-industry-development-with-f5-5g/

[3] White paper on Rf enabling 6G opportunities and challenges from technology to spectrum https://www.6gchannel.com/items/6g-white-paper-rf-spectrum/

[4] 5G high mobility wireless communications: Challenges and solutions. https://ieeexplore.ieee.org/abstract/document/7405718

[5] VIBRATION MONITORING OF A TELECOMMUNICATION BASE STATION BUILDING ACCORDING TO THE STANDARDS DIN 4150-3 AND ETSI EN 300 019-1-3. [Online] https://www.ndt.net/article/defektoskopie2018/papers/11.pdf

[6] Improving vibrotactile pattern identification for mobile devices using perceptually transparent rendering. [Online] https://www.researchgate.net/publication/221270494

https://tsapps.nist.gov/publication/get_pdf.cfm?pub_id=50230

[7] APPLICATION OF SMART MOBILE PHONES IN VIBRATION MONITORING [Online] http://casopisi.junis.ni.ac.rs/index.php/FUMechEng/article/view/887

[8] An autonomous battery-less sensor module powered by piezoelectric energy harvesting with RF transmission of multiple measurement signals. [Online] https://iopscience.iop.org/article/10.1088/0964-1726/18/8/085023

[9] Reducing phase noise degradation due to vibration of crystal oscillators. [Online] https://lib.dr.iastate.edu/etd

[10] Improving vibrotactile pattern identification for mobile devices using perceptually transparent rendering. [Online] https://www.researchgate.net/publication/221270494

[11] Vibration-induced PM Noise in Oscillators and its Suppression. [Online] https://www.researchgate.net/publication/4212754_Vibration-induced_PM_noise_in_oscillators_and_measurements_of_correlation_with_vibration_sensors

[12] Vibration-induced PM Noise in Oscillators and its Suppression. [Online] https://www.researchgate.net/publication/4212754_Vibration-induced_PM_noise_in_oscillators_and_measurements_of_correlation_with_vibration_sensors

[13] Managing Crystal Oscillator Acceleration Sensitivity in Mobile Applications. [Online] https://www.microwavejournal.com/articles/7711-managing-crystal-oscillator-acceleration-sensitivity-in-mobile-applications

[14] PHASE NOISE / JITTER IN CRYSTAL OSCILLATORS. [Online] https://f.hubspotusercontent00.net/hubfs/8153900/Files/Technical%20Documents/PHASE_NOISE_IN_CRYSTAL_OSCILLATORS-1.pdf

[15] Phase-Locked Loop (PLL) Fundamentals. [Online]

https://www.electronics-notes.com/articles/radio/pll-phase-locked-loop/tutorial-primer-basics.php

[16] Vibration-induced PM Noise in Oscillators and Measurements of Correlation with Vibration Sensors1. [Online].

https://tsapps.nist.gov/publication/get_pdf.cfm?pub_id=50230

[17] Network Analyzer [Online] https://en.wikipedia.org/wiki/Network_analyzer_(electrical)

[18] Klaus Nevala ["WR3.4 frequency extenders setup and calibration guide with PNA-X 26,5 GHz"], University of Oulu, 2019.

[19] VDI-707.1-VNAx-Product-Manual (2021) [Online]

https://www.amtechs.co.jp/product/VDI-707.1-VNAx-Product-Manual.pdf

[20] Keysight, Enhanced Response Calibration, (accessed 10 March 2020), [Online].

https://ena.support.keysight.com/e5071c/manuals/webhelp/eng/measurement/calibration/basic_calibrations/enhanced_response_calibration.htm

[21] Frequently Asked Questions- Vector network analyzers

https://www.keysight.com/us/en/products/network-analyzers.html